Iranian Journal of Science & Technology, Transaction B, Engineering, Vol. 32, No. B4, pp 367-383
Printed in The Islamic Republic of Iran, 2008

A SEQUENCE SCHEME TO REDUCE THE RESIDUAL STRESSES IN WELDING OF CIRCULAR ELEMENTS*

S. ZIAEE, M. H. KADIVAR** AND K. JAFARPUR

Dept. of Mechanical Engineering, School of Engineering, Shiraz University, Shiraz, I. R. of Iran
Email: Ziaee@shirazu.ac.ir

Abstract– Accurately predicting welding residual stresses and developing a convenient welding sequence for a weld system is an appropriate task since welding residual stress is inevitably produced in a welded structure. In this work, the effect of layered, block and cascade welding sequences on the thermo-mechanical response of shell weldments is studied by use of a 3-D thermo-viscoplastic model. An Anand model is used to simulate the rate dependent plastic deformation of welded materials. At the same time, modeling of the welded region in the present study has been done on the basis of the "isothermal melting pool" approach. The temperature dependency of the thermal and mechanical properties of materials is considered in the analysis and the effect of the welding speed and welding lag, and the inter-pass temperature is introduced into the model as well. Thus, the model presented here has provided a convenient welding sequence to enhance the fabrication process of a circular weld.

Keywords– Welding sequence, thick shell, Anand model, cascade method, block method, layer method, 3D thermo viscoplastic model

1. INTRODUCTION

Metallurgical welding joints are extensively used in the fabrication industry including ships, offshore structures, steel bridges, and pressure vessels. The merits of such welded structures include a high joint efficiency, water and air tightness, and low fabrication cost. However, residual stresses and distortions can occur near the weld beads due to localized heating by the welding process and subsequent rapid cooling. These high residual stresses in regions near the weld may promote brittle fracture, fatigue, or stress corrosion cracking. Meanwhile, residual stresses in the base plate may reduce the buckling strength of the structure members. Therefore, welding residual stresses must be minimized to control their consequences according to respective requirements. Investigators have developed several methods including heat treatment, hammering, pre-heating, vibration stress relief, and weld sequencing to reduce the residual stresses attributed to welding [1-7]. The in-process control of welding residual stresses becomes more desirable than post-welding rectification or other methods when the manufacturing efficiency is considered. The easiest in-process control method of reducing welding residual stresses is "changing welding sequences".

Various types of sequences are developed and used in practice such as built up, block, back step and the cascade sequence. However, most can be classified into two major categories named multi-pass and multi-block [7]. The selection of proper welding sequences is an important practical challenge in order to reduce residual stresses and distortion. Most studies are centralized on a multi-pass sequence. Teng *et al*. [8] studied the effect of the filling order on residual stresses at an X grove multi-pass butt-weld joint. Mochizuki *et al*. [9] varied the residual stress value by changing the order of welding pass sequences in a

*Received by the editors January 1, 2007; Accepted February 10, 2008.
**Corresponding author

multi-pass fillet weld joint. A two dimensional FE model was used. Nami [7] evaluated the effect of the number of layers on residual stresses in a V grove multi-pass butt-weld.

The prediction of weld residual stresses relies mainly on the accurate prediction of the weld thermal cycle. Oddy et al. [10] stated that the prediction of the temperature field requires a nonlinear, transient, 3D analysis. Studies by Chao and Qi [11] proposed that 3D modeling of the weld process is essential for practical problems and can provide accurate residual stress and distribution results that cannot be obtained from 2D simulations. Many researches have been done on the modeling and analysis of thermal fields in weldments, and various investigators have tried to study the influence of some of the effective parameters such as arc power, welding speed, welding sequences and environmental conditions [1,12-14]. Several models have been developed to simulate the insertion of the arc into the weldments including "Gaussian distortion of heat flux"[15], "double ellipsoidal power density"[16], "ramp heating" [17] and "moving isotherm pool" [18].

The present investigation performs a 3D thermo-viscoplastic analysis using the finite element technique to analyze the thermo-mechanical behavior and evaluate the residual stresses with various types of welding sequences (block, cascade, layered) in circular welded shells. Furthermore, this study provides a convenient welding sequence to improve the fabrication process of circular welded shells. In this study, the arc power and its movement were modeled by assuming that the welded region is an isothermal melted pool. Also, the element "birth" technique to include weld metal deposition effects is employed.

2. MATHEMATICAL MODEL OF WELDING

The Lagrangian description of body motion is used in the formulation of welding as a thermo-mechanical problem for metals. The displacement $\mathbf{u}(\mathbf{X},t)$ and temperature $\theta(\mathbf{X},t)$ in a weld joint are unknown and the initial position of the particle $\mathbf{X}=(X_1^0, X_2^0, X_3^0)$ and the time t are taken as independent variables. The vector joining the point $\mathbf{X}$ and actual position in the space $\mathbf{x}=(X_1^1, X_2^2, X_3^1)$ is the displacement vector given by $\mathbf{u}=\mathbf{X}-\mathbf{x}$. The constitutive variables, i.e. the stress and strain measures used in the Lagrangian formulation, are the second Piola-Kirchoff stress tensor $\mathbf{T}$ and its deviator $\mathbf{S}$, as well as the Green-Lagrange total strain tensor $\mathbf{L}$ and deviator $\mathbf{E}$.

Welding is a coupled thermo-mechanical process and its mathematical model consists of two principles expressing thermal and mechanical equilibrium, i.e. the balance of internal energy and balance of momentum, as well as satisfying initial and boundary conditions. The equilibrium condition for a solid is given by the following equations

$$\begin{aligned} &div(\mathbf{T}+\mathbf{T}\cdot\nabla\mathbf{u})-(\mathbf{b}+\mathbf{r})\rho_0=0 && \text{for particle } \mathbf{X}\in\mathbf{\Omega}\\ &\mathbf{N}\cdot(\mathbf{T}+\mathbf{T}\cdot\nabla u)=\tilde{\mathbf{T}} && \text{for particle } \mathbf{X}\in\partial\mathbf{\Omega}\end{aligned} \tag{1}$$

where $\nabla\equiv N^J\partial/\partial X^J$, and the comma "," is the usual abbreviated notation for a gradient component. The balance of internal energy for a non-rigid conductor can be expressed in the form of

$$\rho\dot{e}+div\mathbf{q}=\mathbf{T}:\dot{\mathbf{L}}+{}_{ext}\mathbf{q}\cdot\mathbf{N}+\rho R \tag{2}$$

where e is the energy density per unit mass, $\mathbf{q}$ is the vector of heat flux transferred through the particle $\mathbf{X}\in\mathbf{\Omega}$, ${}_{ext}\mathbf{q}$ is the heat flux supplied to the welded body through the outer surface $\partial\mathbf{\Omega}$, and R is heat losses through radiation. By considering thermal homogeneity for the welded material and after some manipulations, the indicial form of the equation of the internal energy balance could be rewritten as a function of temperature θ [19]:

$$C\dot{\theta}+K_{IJ}\theta_{,JI}=f_\theta^B+f_\theta^S+\sum_\varsigma F_\theta^\varsigma \tag{3}$$

where

$f_\theta^B = T_{IJ}\dot{L}_{IJ}$	rate of heat generation due to mechanical energy dissipation in weldments
$f_\theta^S = {}_{ext}q_J N_J + \rho R$	heat flux of welding arc and out – fluxes due to convection and radiation
$C = \rho_0 C$	constant volume specific heat
$\sum_\tau \mathrm{F}_\theta^\tau$	concentrated heat fluxes

In the above equation, f_θ^B plays the role of thermo-mechanical coupling between the mechanical and thermal systems. The magnitude of this term in welding is quite small compared to the heat energy of the arc and has a negligible effect on the thermal history of plates [20,21]. Due to this approximation, some investigators have neglected its effect. This assumption causes the problem to be thermo-mechanically uncoupled. Then, two separate analyses, thermal and mechanical, have been performed.

a) Finite element approximation

The finite element method for the fully coupled thermo-mechanical problem is based on the Ritz's approximation of variational equation, i.e. the principle of virtual work and the balance of internal energy [19].

The combined global finite element equation for the fully coupled thermo-mechanical problem is expressed by

$$\begin{bmatrix} \mathbf{K}_u^n & \mathbf{K}_{u\theta}^n \\ \mathbf{K}_{\theta u}^n & \frac{1}{\Delta t}\mathbf{C}^n + \mathbf{K}_\theta^n \end{bmatrix} \begin{bmatrix} \Delta \mathbf{u} \\ \Delta \theta \end{bmatrix}^i = \begin{bmatrix} \mathbf{R}_u^{n+1} \\ \mathbf{R}_\theta^{n+1} \end{bmatrix} - \begin{bmatrix} \mathbf{F}_u^{n+1} \\ \mathbf{F}_\theta^{n+1} \end{bmatrix}^{(i-1)} \tag{4}$$

where $\mathbf{K}_u^n$ is the stiffness matrix corresponding to the mechanical effects, $\mathbf{K}_{u\theta}^n$ is the matrix which transforms thermal energy into a mechanical one, and $\mathbf{K}_{\theta u}^n$ transforms mechanical energy into the thermal one. The thermal stiffness $\mathbf{K}_\theta^n$ is the sum of the stiffness matrix corresponding to conduction, the stiffness related to convection phenomena, and the stiffness associated with radiation effects. $\Delta\mathbf{u}|_{(i)}$ and $\Delta\theta|_i$ are the vector of displacement and temperature increments respectively, $\mathbf{R}_u^{n+1}$ is the vector of externally applied nodal point loads, $\mathbf{F}_u^{n+1}|_{i-1}$ is the vector of nodal point forces equivalent to internal stresses, $\mathbf{R}_\theta^{n+1}$ is the summation of the vectors of nodal thermal loads corresponding to thermal conditions, and $\mathbf{F}_\theta^{n+1}|_{i-1}$ is the vector of nodal thermal loads that correspond to the heat flux through the body surface [19].

The matrixes in equation (2-4) are taken at the current, n+1, and previous, n, time steps and current, (i), and previous, (i-1) iterations at the current time step.

The nonlinear FM system of equations is solved iteratively by the Newton-Raphson scheme.

After neglecting the effect of f_θ^B, the stiffness matrices $K_{\theta u}^n$ becomes zero. This will happen because f_θ^B, which is equal to $\mathbf{T}:\dot{\mathbf{L}}$, plays the role of thermo-mechanical coupling between the mechanical and thermal systems. The uncoupled finite element equations for the thermo-mechanical problem is then obtained after f_θ^B is omitted.

b) Mechanical model

If transient thermal stresses produced in welding are completely elastic and no incompatible strains are formed, no residual stresses will remain. However, plastic strains are formed in the region around the weld. In this region, the temperature rapidly increases and nearly reaches the melting point of the material.

At high temperatures the yield strength of metals reduces. Therefore, transient thermal stresses exceed the yield point of the material, and weldment undergoes plastic deformation. In addition, material is at a high homologous temperature in this region, and experiencing rapid temperature changes could result in a high thermal strain rate. Thus, rate dependent effects are relatively significant. For these reasons, a thermoelastic-viscoplastic model is used to simulate the material behavior.

A simple set of constitutive equations for large, isotropic, visco-plastic deformations is the single-scalar internal variable model proposed by Anand [22]. Two basic features exist in the Anand model. First, this model needs no explicit yield condition and no loading-unloading criterion. Second, this model employs a single scalar as an internal variable to represent the averaged isotropic resistance to plastic flow. The inelastic strain rate $\dot{E}^P$ for the Anand model is defined by [19]:

$$\dot{\mathrm{E}}^{\mathrm{P}} \equiv \tilde{\dot{\mathrm{E}}}^{\mathrm{P}}(\mathrm{S},\mathrm{z}_1) = \dot{\varepsilon}^{\mathrm{P}} \frac{\mathrm{S}}{\|\mathrm{S}\|}$$

$$\dot{\varepsilon}^{\mathrm{P}} = \tilde{\dot{\varepsilon}}^{\mathrm{P}}(\mathrm{S},\mathrm{z}_1) = \mathrm{A}\exp\left(-\frac{\mathrm{Q}}{\mathrm{R}\theta}\right)\left[\sinh\left(\xi\frac{\|\mathrm{S}\|}{\mathrm{z}_1}\right)\right]^{\frac{1}{\mathrm{m}}} \tag{5}$$

where the constitutive function $\tilde{\dot{\varepsilon}}^{P}$ was proposed by Anand [22]. Evolution equations for the internal variable z_1 are given by [19]:

$$\dot{z}_1 = h_0\left[1-\frac{z_1}{z^*}\right]^a \dot{\varepsilon}^P \qquad for \quad z_1 \le z^*$$

$$\dot{z}_1 = -h_0\left[\frac{z_1}{z^*}-1\right]^a \dot{\varepsilon}^P \qquad for \quad z_1 \succ z^* \tag{6}$$

with the criterion number

$$z^* = \bar{z}\left[\frac{\dot{\varepsilon}^P}{A}\exp\left(-\frac{Q}{R\theta}\right)\right]^{\eta}$$

where $A, Q, \xi, m, z, h_0, a, \bar{z}$, and η are constants of the Anand model, and R is the Boltzman's constant. The material constants for the Anand model, which are used in the present work, are listed in Table 1.

The stiffness matrix corresponding to mechanical effects, $\mathbf{K}_u^n$ (equation (2-4)), consists of linear, $\mathbf{K}_L^n$, and nonlinear, $\mathbf{K}_{NL}^n$, stiffness matrixes. The linear and nonlinear stiffness matrixes are defined by [19]

$$\mathbf{K}_L^n = \int_{V_0}\left[\mathbf{B}_L^n\right]^t \hat{\mathbf{C}}\mathbf{B}_L^n dV$$

$$\mathbf{K}_{NL}^n = \int_{V_0}\left[\mathbf{B}_{NL}^n\right]^t \hat{\mathbf{T}}\mathbf{B}_{NL}^n dV \tag{7}$$

where $\mathbf{B}_L^n$ and $\mathbf{B}_{NL}^n$ are the linear and nonlinear strain displacement respectively, $\hat{\mathbf{T}}$ is the matrix representation of the second Piola-Kirchoff stress, and $\hat{\mathbf{C}}$ is the consistent or algorithmic tangent modulus which has to be defined for each material model as the $\left[\frac{\partial \mathbf{T}}{\partial \mathbf{L}}\right]$ contribution to the global stiffness matrix [19]. In order to obtain $\hat{\mathbf{C}}$, residual functions are expressed in the form of [19]

$$F(\mathbf{S},z) \equiv \mathbf{S}^{n+1}\big|_i - {}^*\mathbf{S}^{n+1} + 2\Delta t\mu[\dot{\varepsilon}^p]^{n+1}\big|_i \frac{\mathbf{S}^{n+1}}{\|\mathbf{S}\|_M} = 0$$

$$G(\mathbf{S},z) \equiv z^{n+1}\big|_i - z^n - \Delta t\dot{z} = 0 \tag{8}$$

where ${}^{*}\mathbf{S}^{n+1}$ is the elastic deviator and $\|\mathbf{S}\|_M$ is the Mises equivalent stress equal to $(3/2)^{1/2}\|\mathbf{S}\|$ with the natural norm defined by $\|\mathbf{S}\| = (\mathbf{S}:\mathbf{S})^{1/2}$.

The Newton-Raphson method is used to solve residual equations and is found to be $\mathbf{S}^{n+1}$ and z^{n+1} simultaneously. Then by using the updated total stress tensor (Eq. (2-9)) the consistent tangent modulus is updated:

$$\mathbf{T}^{n+1} = \mathbf{S}^{n+1} + \frac{1}{3}\mathbf{q}tr^{*}\mathbf{T}^{n+1} \tag{9}$$

where ${}^{*}\mathbf{T}^{n+1}$ is elastic predictor and $\mathbf{q}$ is $[1 \quad 1 \quad 1 \quad 0 \quad 0 \quad 0]^{t}$ [19].

Table 1. Constants of Anand's viscoplastic model for the selected material [7]

Parameter	Value	Unit	Represent:
z	102.7	Mpa	Initial value of deformation resistance
Q/R	$\frac{312.35}{8.314}$	$\frac{\text{KJ/mole}}{\text{KJ/mole}^{\circ}\text{K}}$	$\frac{\text{Activation energy}}{\text{Universal gas content}}$
A	6.346e11	Sec^{-1}	Pre-exponential factor
ξ	3.25	Dimensionless	Multiplier of stress
m	0.1956	Dimensionless	Strain rate sensitivity of stress
h_0	3093.1	MPa	Hardening/softening constant
$\bar{z}$	125.1	MPa	Coefficient for deformation resistance saturation value
η	.06869	Dimensionless	Strain rate sensitivity of saturation value
a	1.5	Dimensionless	Strain rate sensitivity of hardening/softening

c) Thermal model

Because of the small size of the melted region (weld pool), the variation of temperature through the pool has a negligible effect on the thermal history of the joining plates. In other words, the temperature of the welding pool is assumed to be uniform and is taken as the melting temperature of the welded materials. Due to this assumption, in this work the arc power and its movement were modeled by assuming that the welded region is an isothermal melted pool having a constant temperature and location that discretely changes with respect to time. In this way, the length of each welded layer, or each welded block, is divided into a number of parts and, according to the welding sequence, the location of the melted pool is changed with respect to time. The applied heat is then injected into the weldments in the moving weld pool and transferred from its boundary to the other regions by conducting through the solid materials and convection to the surroundings. For a short time during welding, the welded region remains red-colored and a portion of the heat is also dissipated by radiation. In comparison to the two other modes of heat transfer, the part of the arc power transferred by radiation is small [21], so the effect of this mode of heat transfer is neglected in this study.

Welding time in this work is calculated by dividing the welder speed obtained from the practical welding characteristic data over the length of the welded region. The welding lag, inter-pass temperature and the temperature dependent thermal properties of the material were also incorporated into the model (Table 2).

Table 2. Variation of material thermal and mechanical properties with temperature [7]

Temperature, T ($^{\circ}$C)	Thermal conductivity, k ($Wm^{-1}K^{-1}$)	Specific heat, C_{ρ} ($Jkg^{-1}K^{-1}$)	Coeff. of thermal expansion (10^{-6+}/C)	Young's modulus E(GPa)
0	51.9	450	10	200
75	-	486	-	-
100	51.1	-	11	200
175	-	519	-	-
200	49	-	11.5	200
225	-	532	-	-
275	-	557	-	-
300	46.1	-	12	200
325	-	574	-	-
375	-	599	-	-
400	42.7	-	-	-
450	-	-	13	150
475	-	662	-	-
500	39.4	-	-	-
550	-	-	14	110
575	-	749	-	-
600	35.6	-	14	88
675	-	846	-	-
700	31.8	-	-	-
725	-	1432	14	20
775	-	950	-	-
800	26	-	14	20
1000	27.2	-	14.5	11
1200	-	-	15	2
1500	29.7	400	15	.2

d) Element birth technique

If material is added to (or removed from) a system, certain elements in the model may become "existent" (or "nonexistent"). The element birth and death options can be used to deactivate or reactivate selected elements in such cases. To achieve the "element death" effect, material properties are nullified by the program. In like manner, when elements are "born", they are reactivated by attributing normal values to their properties.

In this work, the weld elements in front of the weld are always kept inactive until the front border of the heat source enters the element in the thermal analysis. The element is activated at melting point temperature in the thermal analysis. In the mechanical analysis the elements are kept inactive until the front border of the heat source has passed the inactive element by about one element length. In this analysis, the element is activated with very soft properties (material property at melting point temperature).

e) Model validation

To confirm the accuracy of the present method, a specimen was constructed using multi-pass butt-welding with a length, width and thickness of L=30mm, W=100mm, t=4.5 mm, respectively. Pass sequences and welding speed are shown in Table 3. Figure 1 portrays the distribution of the longitudinal residual stress on the plate. Based on the proposed model, Chang and Teng [23] provided experimental results for this test-case. The results of the presented method are in good agreement in comparison with the experimental data.

Table 3. Welding speed for each pass [23]

Pass No.	1	2	3
Speed (mm/s)	1	0.75	0.55

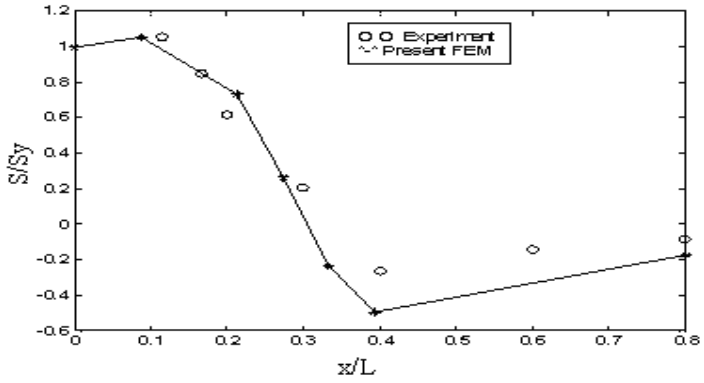

Fig. 1. Comparison between the longitudinal residual stress distribution of the present method and experimental data of [23]

3. COMPUTATIONAL MODEL

On the basis of industrial consultation, a circular path is selected to study the effect of different kinds of welding sequences on the thermo-mechanical response of weldments. Industrial observation shows that the use of a layered (built-up) method is sometimes unprofitable in large circular paths joints, and crack growth is sometimes seen near the weld seam [24]. So the use of other welding sequences is desirable to overcome this difficulty. Therefore, in this study, the junction of a pipe to a spherical cap (the circular section of sphere) is modeled using different welding sequences.

Figure 2 illustrates a pipe and a spherical cap shell jointed by butt-weld. The thickness and inner diameter of the pipe and spherical section are assumed to be 12, 203.2, and 4000 mm, respectively. The mechanical properties are dependent on the temperature history as listed in Table 1. This model (Fig. 2) was constructed by approximately 15000 elements. The size of the elements in the regions with high temperature gradients was chosen to be small, while the dimension of other elements increases as the distance from the joint centerline increases.

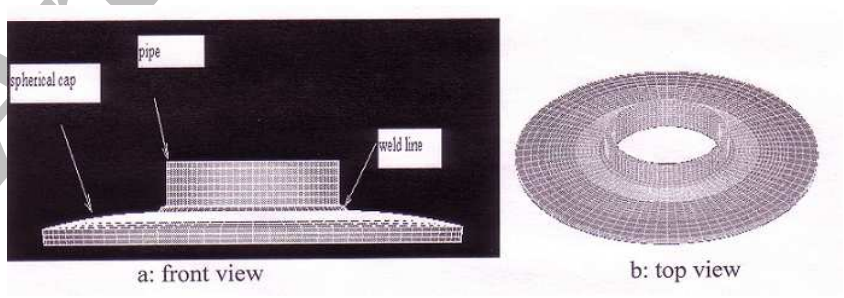

Fig. 2. Finite element mesh of pipe, spherical cap and weld bead

Various types of sequences are developed such as built up, block, back step and cascade sequence (Fig. 3). As Fig. 3 shows, three different sequences can be used to weld thick plates. One of them is called "built-up". In this method the thickness of the grove is divided into a number of divisions and each part is subdivided further in the transverse direction (Fig. 4c). Then each part is welded along the entire weld length on the base of a suitable order.

If the length of the weld seam is divided into a number of divisions and each division (with a convenient order) is completely welded based on the "build-up" method, the weld-type is known as "block sequence" (Fig. 4b).

In the cascade method, the length and thickness of the weld seam are divided into a number of divisions such as the block method. The welding is started from the first block and the first layer of the first block is welded. The second layer is composed of the second layer of the first block and the first layer of the second block. The 3rd layer is made of the 3 rd layer of the first block, the 2nd layer of the second block and the first layer of the 3 rd block. After filling each block, a similar procedure continues with the next block. This procedure is shown in Table 4 for the three first layers and the three first blocks (Fig. 4d).

Table 4. Cascade procedure for the 3 first layers and the 3 first blocks

No. pass	1	2	3
No. block/No. layer	1/1	1/2 and 2/1	1/3 and 2/2 and 3/1

Three different kinds of welding sequences, i.e. block, built-up and cascade sequences are used in this work. With using the “lump pass” technique [8] the built-up sequences are simplified as a layer method. Figure 4 depicts how the joint was welded by these sequences in this research. Two different block sequences are proposed. In the first type, after completing the first block, the model was permitted to cool down to near ambient temperature, and the second block was then welded (This is called sequential block cooling). In the second, after completing the first block, the second block was immediately welded (This is called the continuous block method).

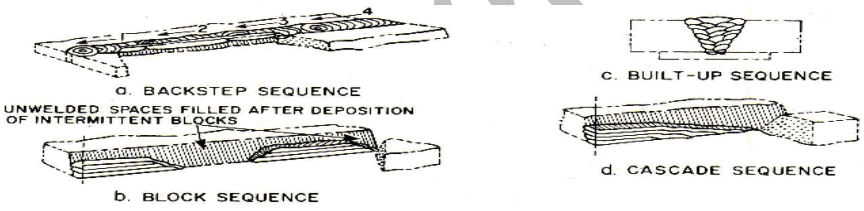

Fig. 3. Some different kind of welding sequences [25]

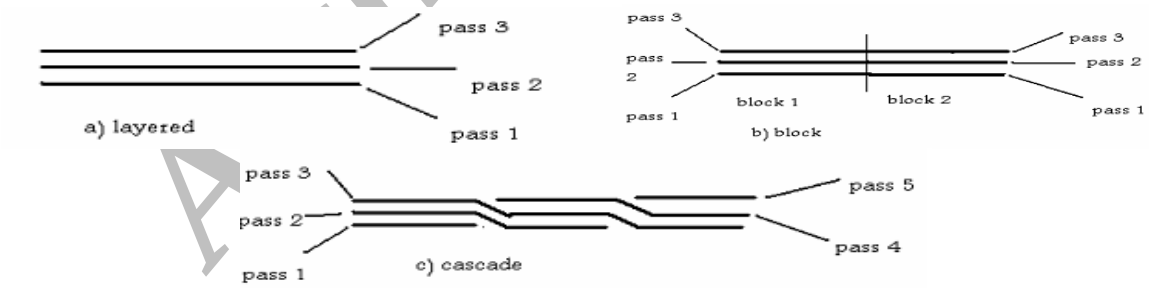

Fig. 4. Welded method according to industrial consultant

4. RESULTS

The temperature profile of points near the weld toe greatly depends on the position of the points and the kind of welding sequences. Moreover, the fluctuation of the temperatures, the value of the maximum temperature and its time of reach can be quite different as the welding sequences change. For example, Fig. 5 reveals that the cascade method, in comparison with the layered method, experiences a lower fluctuation of temperature over a longer time and a smaller value of the maximum temperature at the starting point of welding. Figure 6 illustrates that the cascade method does not show any fluctuation with

respect to the continuous block method in the 180 degree line with respect to the starting point of the welding; though some similarities can be seen in some paths (Fig. 7).

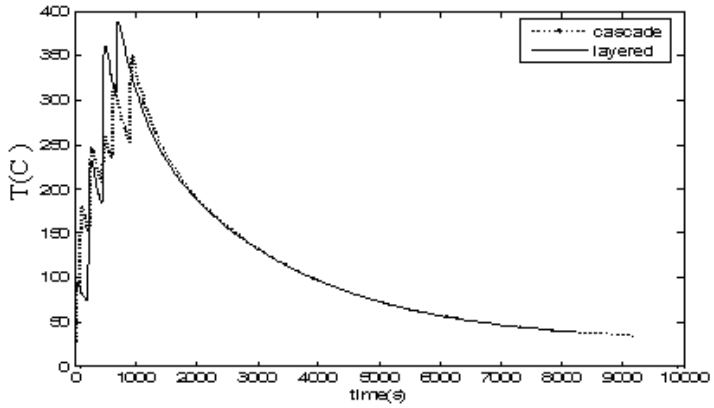

Fig. 5. Comparison between temperature history of cascade and layered methods in starting point of welding

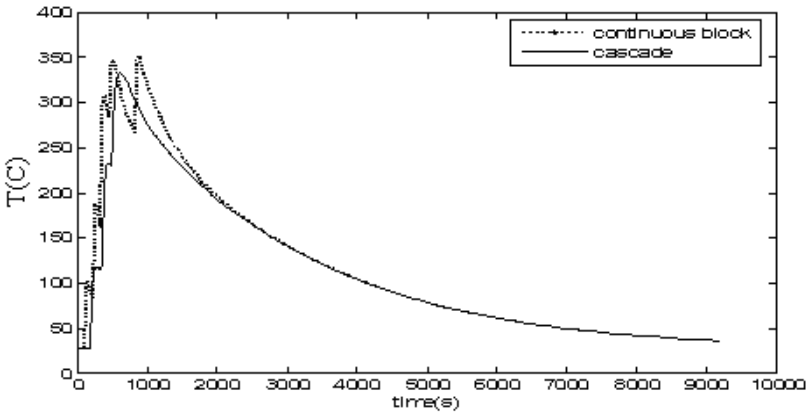

Fig. 6. Large differences can be seen between temperature histories of continuous block and cascade methods in 180 degree line with respect to the starting point of welding

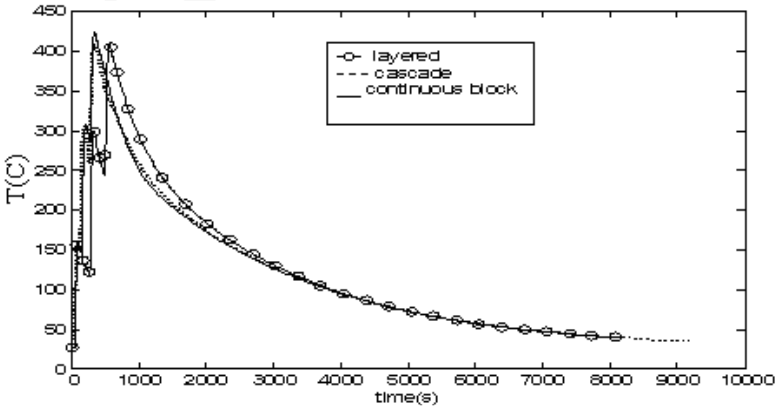

Fig. 7. Comparison between temperature histories of cascade, layered and continuous block methods in 270 degree line with respect to starting point of welding

Temperature history greatly affects the stress history. Figure 8 illustrates the temperature and stress variation with respect to time for a point on the spherical cap near the weld toe for cascade and layered methods. As this figure reveals, the magnitude of stress decreases with decreasing the temperature and

vise versa. At the end of fluctuations, 200 seconds before the start of the cooling stage of the cascade method, the cooling stage of the layered method has started. So, the stress at the time of the starting point of the cascade cooling stage is more negative for the cascade method than the layered. Therefore, the stress of the cascade method starts to increase 200s later. On the other hand, the rate of increasing stress is the same for both methods and they will reach a stable value of stress at the same time (4500s) and temperature (60^0C). This behavior results in minimizing the transverse stress of the cascade method (Fig. 8).

Similar discussions can be given when comparing the temperature and stress history of a continuous block with the layered method and cascade with the continuous block method.

Contrary to the cascade, layered, and continuous block methods, the graphs of the sequential block cooling method reveals the fact that when each block was completely welded (after welding each block, it was permitted to be cooled), symmetrical points, with respect to the pipe-axis, have similar symmetrical behavior regarding the start time of the second block (Fig. 9).

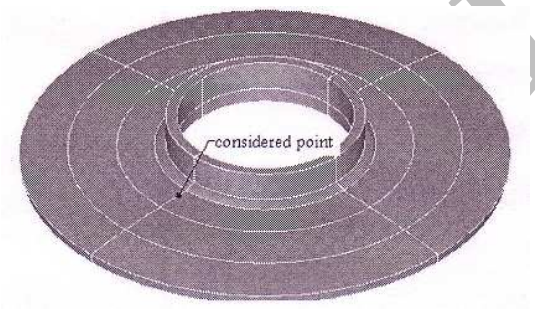

Fig. 8a: Position of considered point

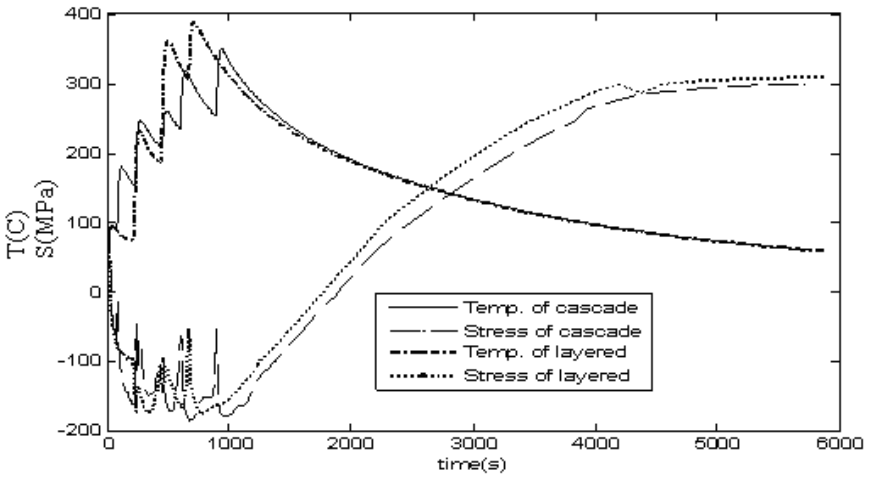

Fig. 8b: Comparison between temperature and stress history for cascade and layered method.

The magnitude of produced residual stresses, after completing the first block at sequential block cooling, is lower than the generated residual stresses after finishing the welding at the other three methods (layered, cascade and continuous block) because of less welding [12]. When the second block is started, renewed heating of the cooled zone decreases the stresses, and after completing the second block, the stresses do not grow more than their initial value (which are produced after cooling the first block) in the first half of the joint. The value of transverse stresses (perpendicular to weld seam) are compared in Table 5 for a particular point for different kinds of welding sequences. The stress history of this point can be seen in Figs. 8 and 10 for layered, cascade and sequential block cooling methods.

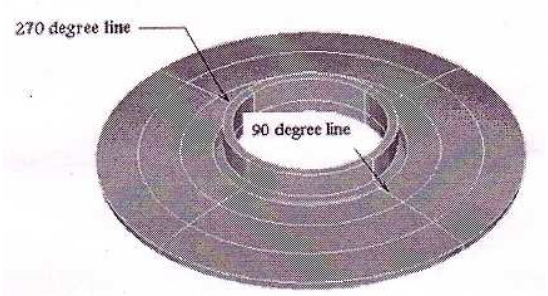

Fig. 9a. Position of considered lines

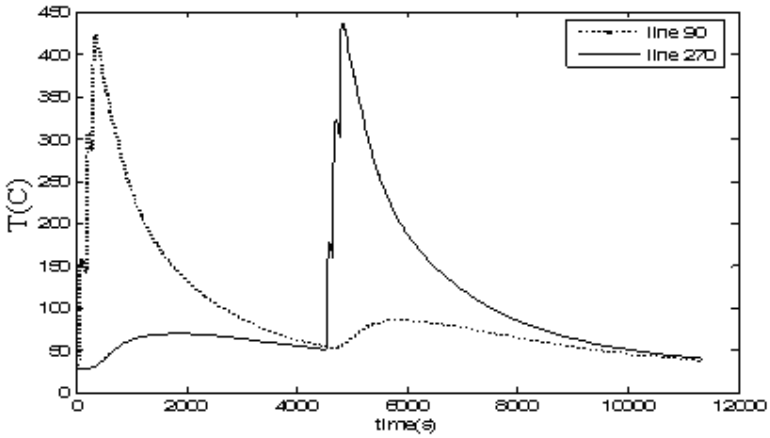

Fig. 9b: Comparison of temperature distribution versus time relating to starting point of welding in sequential block cooling method

Table 5. Comparison between final residual stresses at a particular point for different kinds of sequences

Welding sequence	Sequential block cooling finishing of first block / second block		Layered	Cascade	Continuous block
Stress(MPa)	200	201.3	311	300	299

Obviously, the cooling stage between the two blocks of the sequential block cooling method leads to a noticeable decrease of stress, especially in the first half of the joint (Fig. 8,10 and Table 5).

Figure 11 depicts the pattern of circumferential stress (parallel to weld seam) at the weld toe. Though similar stress distribution can be seen for the two halves of the joint, the magnitude of stress related to the second half of the welding joint is more than the first half of the welding joint; the figure shows an increase of nearly 25%. Initial pre-stress and the reduction of joint flexibility due to welding the first block may cause this behavior. This trend repeats for transverse stresses around the weld toe**.**

The variation of stress components is compared for four different kinds of welding sequences near the weld toe in Fig. 12. The position of the considered points is shown in Fig. 12a. On the basis of Fig. 12b, though there is a negligible difference between the magnitudes of produced circumferential stress by cascade, continuous block and layered methods near the weld toe on the spherical cap, a 5% reduction is seen for the cascade and continuous block compared to the layered method on the pipe. As Fig. 12b shows, the difference between the stress magnitude of sequential block cooling and the layered method is significant. A comparison between the magnitude of circumferential stress for sequential block cooling and layered methods reveals a decrease of 35% in the spherical cap and 55% at the weld toe in the pipe for the sequential block cooling method (Fig. 12b). These differences reduce when the distance from the weld

toe is increased (Fig. 12b). Similar behavior can be seen in Fig. 12c that compares the variation of transverse stresses near the weld toe for different kinds of welding sequences, although a decrease of 8% is seen for the cascade and continuous block compared to the layered method on the spherical cap (Fig. 12c).

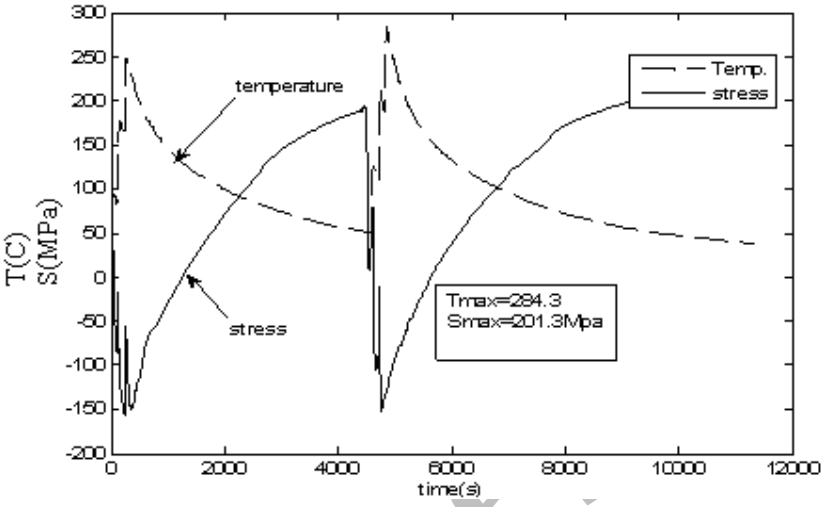

Fig. 10: Variation of temperature and stress versus time of sequential block cooling method in starting point of welding

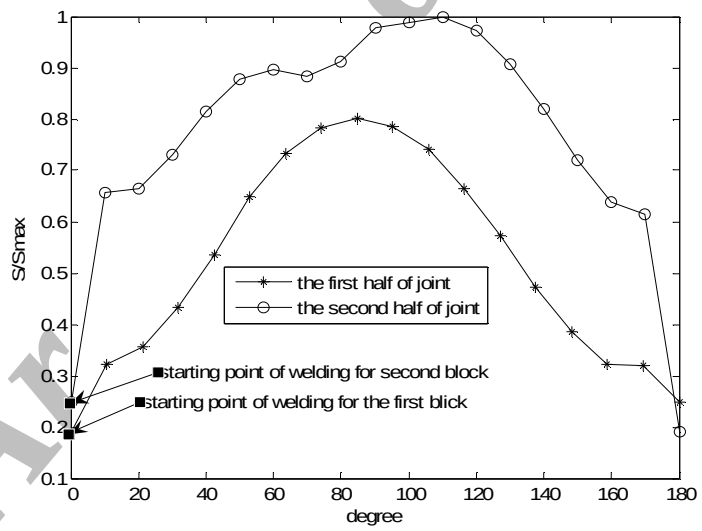

Fig. 11. Distribution of circumferential stress around the weld toe. Vertical axe shows the ratio of stress to its maximum value

A similar discussion can be given for different lines with respect to the starting point of welding. High tensile residual stresses near the weld toe are important to calculate fatigue strength or the crack-grow resistance of weldments and their reduction near the weld is desirable [25, 8]. On the basis of Fig. 12, one can conclude that the use of the sequential block cooling method increases the crack-grow resistance and the fatigue strength of weldments.

Figure 13 shows the variation of stresses along the length of the pipe. It is seen that the difference between stresses produced by the sequential block cooling method and the other three methods (layered,

cascade and continuous block cooling) decreases when the distance from the weld toe is increased, and increases again near the end. Thus, sequential block cooling produces the lowest compressive stress near the end of the pipe. Although negative stresses improve fracture and fatigue strength, they decrease the stability of the structure (of course this phenomenon is not important in thick weldments). Obviously, the risk of buckling is lower if sequential block cooling is used to weld.

Variations of von Mises stress on the circular path of the spherical cap are presented in Fig. 14. This figure illustrates that the sequential block cooling sequence has not only generated a symmetrical residual stress profile with respect to the 180 degree line, but it has the smallest value as well. As this figure shows, the patterns of residual stress produced by cascade, layered and continuous block methods are similar. Figure 14 also verifies that the difference between the magnitudes of von Mises residual stresses increases for cascade, layered and continuous block methods near the edge (Fig. 14b).

Figure 15 shows the final shape of the pipe in the horizontal plane. Clearly the sequential block cooling method has generated symmetrical deformation. Also, this method deforms the pipe more than other methods.

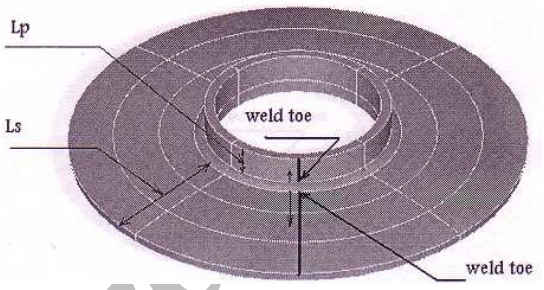

Fig. 12a: The position of considered lines along spherical cap and pipe is shown by thick black lines

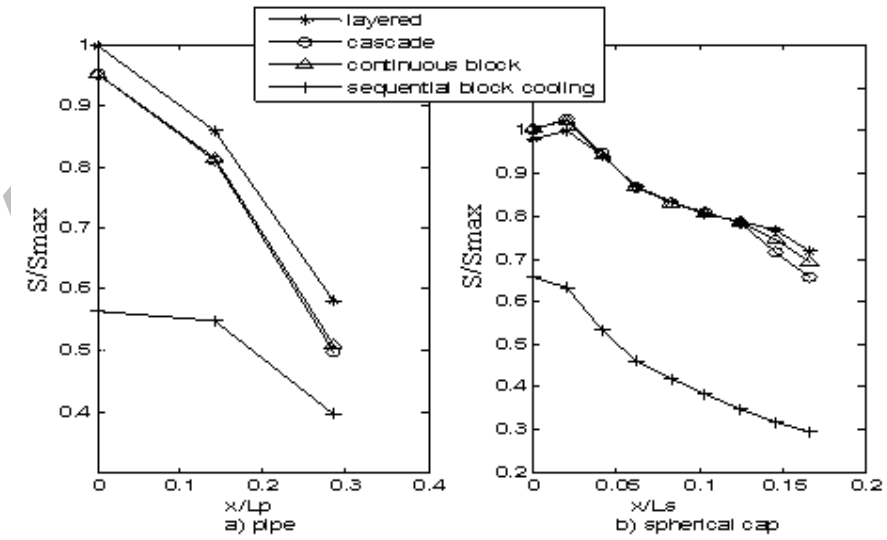

Fig. 12b. Variation of circumferential stress near the weld toe. Vertical axis showns the ratio of stress to maximum stress produced by layered method in each part

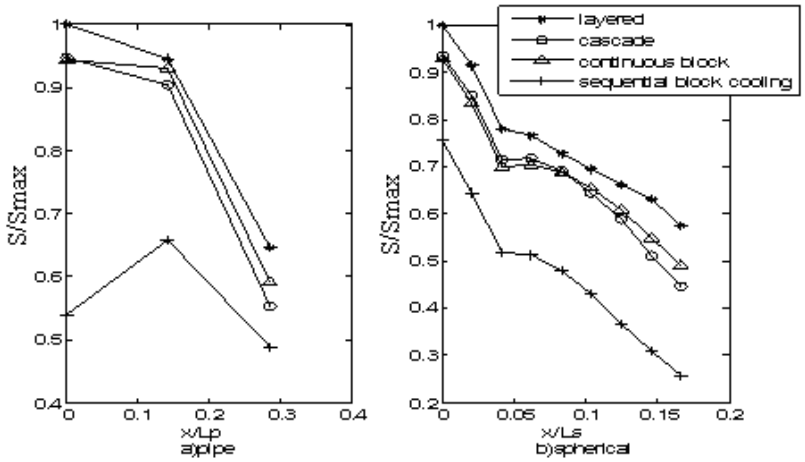

Fig. 12c. Variation of transverse stress near the weld toe. Vertical axis shows the ratio of stress to maximum stress produced by layered method in each part

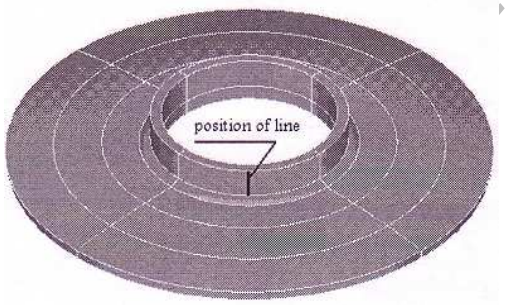

Fig. 13a. Position of line along the pipe

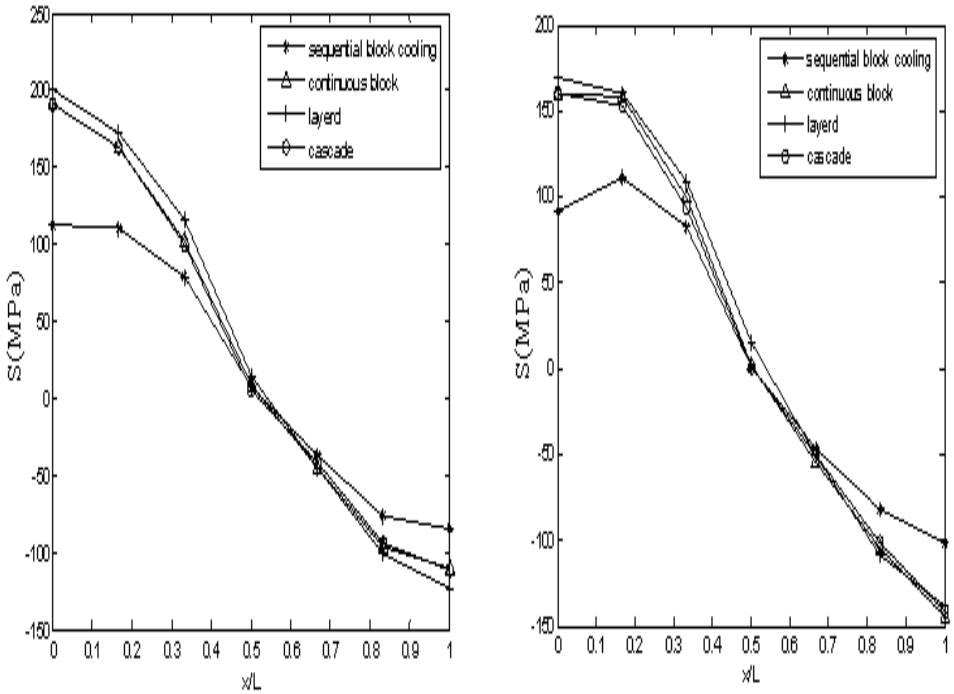

Fig. 13b. Distribution of circumferential and radial stresses on the pipe on the basis of cylindrical coordinate. Horizontal axis is the ratio of distance from the weld toe to the length of pipe

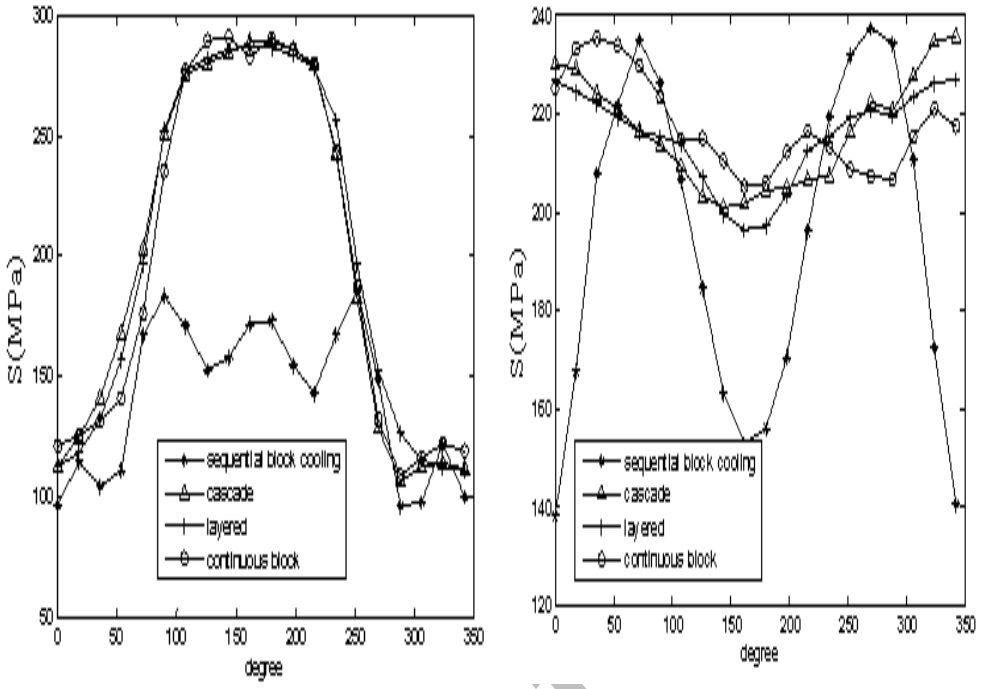

a) Near weld toe b) Near edge

Fig. 14. Distribution of Von-Mises stress on spherical cap with respect to the position of points on a circular path

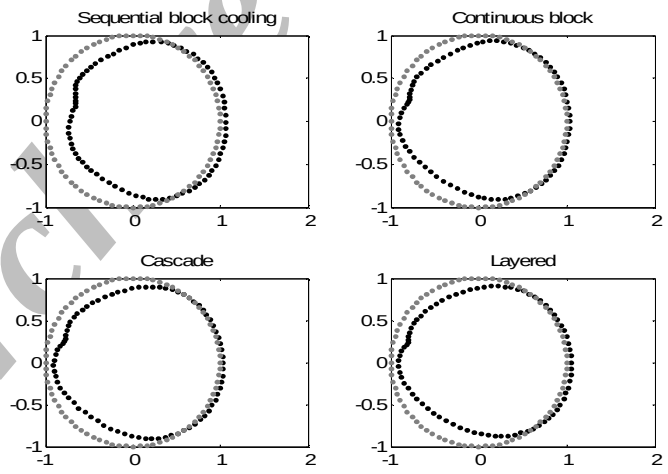

Fig. 15. Final shape of pipe opening for different kinds of welding sequences. The shape of pipe before and after welding is presented by gray and black dots respectively

5. CONCLUSION

The effect of different welding sequences (sequential block cooling, layered and cascade, continuous block) on residual stresses and distortions are evaluated and the following conclusions can be drawn:

1- Cascade and continuous block sequence produce a smaller magnitude of transverse stress near the weld toe than the layered sequence. The reduction of stress on the pipe is more than the spherical cap.

2- Though the magnitude of circumferential stress is decreased on the pipe when cascade or continuous block is used instead of the layered method, there is no noticeable difference between the magnitude of circumferential stresses produced by cascade, continuous block and layered methods near the weld toe on the spherical cap.
3- The use of sequential block cooling leads to a noticeable decrease of stresses near the weld toe. The reduction of circumferential stress is more than the transverse stress on the spherical cap.
4- The difference between the magnitudes of stresses produced by different kinds of welding sequences reduces with increasing distance from weld toe.
5- The smallest magnitude of compressive stress produced near the edge of the pipe and spherical cap belongs to sequential block cooling.

Thus, due to its lowest magnitude of residual stresses, the results clearly show that the use of the sequential block cooling sequence is better than other methods (layered, continuous block and cascade methods), though it produces more deformation.

REFERENCES

1. Pilipenko, A. (2001). Computer simulation of residual stress and distortion of thick plates in multi-electrode submerged arc welding, their mitigation techniques. Ph.D. Thesis, Norwegian University of Science and Technology, Trondheim, Norway.
2. Nakacho, K. & Ueda, Y. (1996). A simple estimating method for reduction of welding residual stresses in thick welded joint from stress-relief annealing-Part I: Development of the analytical method for relaxation tests and its applicability. *Journal of Pressure Vessel Technology*, pp.343-350
3. Jonassen, F., Meriam, J. L. & Degarmo, E. P. (1946). Effect of certain block and other special welding procedures on residual welding stresses. *Welding Journal 25*, Vol. 9, pp 492s-496s.
4. Rybicki, E. F. & Mcguire, P. A. (1985). The effect of induction heating conditions on controlling residual stresses in welded pipes. *Journal of Engineering Technology*, Vol. 107, pp. 148-153.
5. Ueda, Y., Nakacho, K. & Shimizu, T. (1986). Improvement of residual stresses of circumferential joint of pipe by heat-sink welding. *Journal of Pressure Vessel Technology*, Vol. 108, pp. 14-23.
6. Chou, C. P. & Lin, Y. C. (1992). Reduction of residual stresses by parallel heat welding in small specimen of Type 304 stainless steel. *Mater. Sci. Technol. 8*, pp. 179-183.
7. Nami, M. R., Kadivar, M. H. and Jafarpur, K. (2004). 3D thermo-viscoplastic modeling of welds: effect of pice-wise welding on thermo-mechanical response of thick plate weldments. *Iranian Journal of Science and Technology, Transaction B*, Vol. 28, No. B4, pp. 467-478.
8. Teng, T. L., Chang, P. H. & Tseng, W. Ch. (2003). Effect of welding sequences on residual stresses. *Computers and Structures*, Vol. 81, pp. 273-286.
9. Mochizuki, M., Hattori, T. & Nakakado, K. (2000). Residual stress reduction and fatigue strength improvement by controlling welding pass sequences. *Transaction of the ASME*, Vol. 122, pp. 108-112.
10. Oddy, A. S., Goldak, J. A. & McDill, J. M. J. (1989). Transformation plasticity and residual stresses in single-pass repair welds. ASME PVP-Weld residual stresses and plastic deformation, Vol. 173, pp. 13-18.
11. Chao, Y. & Qi, X. (1999). Thermo-mechanical modeling of residual stress and distortion during welding process, ASME PVP-Fracture. *Fatigue and Weld Residual Stress*, Vol. 393, pp. 209-213.
12. Pattee, F. M. (1975). Buckling distortion of thin aluminum plates curing welding. M.S. Thesis, Massachusetts Institute of Technology.
13. Lin, Y. C. & Lee, K. H. (1997). Effect of welding parameters on the residual stress by the parallel heat welding. *Int. J. of Pressure Vessels and Piping*, Vol. 71, No. 2, pp. 197-202.

14. Baradaran, GH. H. (2000). In plane thermoelastic-viscoplastic modeling of arc welding with special reference to optimization of welding sequences. Ph.D. Thesis, Shiraz University, Shiraz, Iran.
15. Pavelic, V., Tanbakuchi, R., Uyehara, O. A. & Myers, P. S. (1969). Experimental and computed temperature histories in gas tungsten- arc welding of thin plates. *Welding Journal*, Vol. 48, 7, pp. 295-305.
16. Goldak, J., chakravarti, A. & Bibby, M. (1984). A new finite element model for welding heat source. *Metallurgical Transactions B*, Vol. 15B, pp. 299-305.
17. Shim, Y., Feng, Z., Lee, S., Kim, D., Jaeger, J., Papritan, J. C. & Tsai, C. L. (1992). Determination of residual stresses in thick section weldments. *Welding Journal*, September, pp. 305s-312s.
18. Goldak, M. Gu., & Hughes, E. (1993). Steady state thermal analysis of welds with filler metal addition. *Can. Mettall. Q*., Vol. 32, pp. 49-55.
19. Ronda, J. & Oliver, G. J. (1998). Comparison of applicability of various thermo-viscoplastic constitutive models in modeling of welding. *Comput. Methods Appl. Mech. Engrg*., Vol. 153, pp. 195-221.
20. Argyris, J. H., Szimmat, J. & William, K. J. (1982). Computational aspects of welding stress analysis, *Comput. Methods Appl. Mech. Engrg*., Vol. 33, pp. 635-666.
21. Hong, J. K., Tsai, C. L. & Dong, P. (1998). Assessment of numerical procedure for residual stress analysis in multi-pass welds. *Welding Journal*, pp. 372s-382s.
22. Brown, S. B., Kim, K. H. & Anand, L. (1989). An Internal variable constitutive model for hot working of metals. *International Journal of Plasticity*, Vol. 5, pp. 95-130.
23. Chang, P. & Teng, T. (2004). Numerical and experimental investigations on the residual stresses of the butt-welded joints. *Computational Material Science*, Vol. 29, pp. 511-522.
24. Mosavi, J. (2005). Welding engineer of petrochemical industries design and engineering company (PIDEC). Personal Contact .
25. Masubuchi, K. (1980). *Analysis of welded structures*. Pergamon Press Ltd.